

Peculiarities of Compact Surface-Plasma Sources Operation (Practical Aspects)

Vadim Dudnikov

Brookhaven Technology Group, Inc., NY, USA

ABSTRACT

Operation Experience of Compact Surface-Plasma Sources (CSPS) under operation in different laboratories around the World is considered. The CSPS have high plasma density, high emission current density. They are very small, simple and effective, have a high brightness in noiseless mode of operation, and high pulsed gas efficiency. The CSPS are very good for pulsed operation and continues operation during many months has been achieved. Negative ion formation, charge-exchange cooling of H⁻ below 1 eV, high brightness beam extraction, formation, transportation, space charge neutralization, brightness preservation instability dumping are discussed. Practical aspects of SPS design, simulation and operation, pulsing a gas and cesium admixture control, lifetime enhancement of selected SPS are described and compared.

Features of CSPS are small volume, small gaps between electrodes, high plasma density and high emission current density. These features have complicated the long time operation of CSPS with high beam parameters, because a sputtering rate, flakes formation, deposition of insulators surface and probability of short circuit of electrodes should be high. But in many versions of CSPS very long operation time was reached. Features of CSPS important for long time operation are considered.

INTRODUCTION

Through the development of Charge Exchange Injection [1] and Surface Plasma Sources (SPS) with Cesium Catalysis [2,3,4,5,6] the possibility for the accumulation of a high brightness proton beam in circular accelerators was increased greatly, and now it is more than sufficient for all real applications. The combination of the SPS with charge-exchange injection improved large accelerators operation and has permitted beam accumulation up to space-charge limit and **overcome** this limit several times [6]. The early SPS for accelerators have been in operation without modification for ~25 years. In this note an attention is concentrated on the seldom-discussed distinctive features of high brightness beam formation in noiseless regimes of negative ion source operation. Beam quality enhancement up to the level $j/T > 1$ A/cm²eV is possible by optimization of negative ion generation, extraction, and transportation in SPS with cesium catalysis. Advanced version of the SPS for accelerators will be described. Features of negative ion beam formation, transportation, space-charge neutralization- overneutralization, and instability damping will be considered. Practical aspects of SPS operation and high brightness beam production will be discussed.

One practical result of development of high brightness negative ion source is accepting of the charge-exchange injection in circular accelerators for a routine operation.

Today, negative ion sources are the *Source of life* for gigantic accelerator complexes such as FNAL, BNL, DESY, KEK..., for pulsed neutron sources, for many synchrotrons and storage rings. The efficient and reliable operation of negative ion sources is largely

responsible for the productivity of these facilities. Many discoveries in high-energy and solid physics were made as a direct result of using the SPS negative ion source. The rapid development of high brightness H^- sources was stimulated by the first success of high current proton beam accumulation using charge-exchange injection [1]. Research in this area was supported by the interest in “Star Wars” [7]. In fact, these defense interests were also the main reason for the long delay of the first publication of results. Nonofficial communication, however, was relatively fast. Main early works in SPS development have been collected in report [8].

For the past several years, laboratories in many countries around the world have had research programs to develop negative ion sources with upgraded characteristics but up to now they have not resulted in a source that can deliver the desired parameters. Ion sources requirements for new projects and a status of ion sources developments are collected in review of R. Scrivens [9].

Until 1971 a main attention was concentrated on the charge-exchange ion sources, because was no hope to extract from the plasma directly more than 5 mA of H^- . After first observation of a strong increasing of negative ion production following a small admixture of cesium into the gas discharges [2,3,4], and development of a first SPS for accelerators [5] has been start very fast development and adaptation of SPS in many USA laboratories, in Europe and in Japan, and International Symposiums for Production and Neutralization of Negative Ions and Beams has been established [10]. Now the Surface Plasma Method of negative ion production and SPS considered in many books (recently in book [11]). Good review of SPS for accelerators presented in reports of J. Peters [12]. Production of polarized negative ions by charge- exchange with a slow negative ion in SPS has been proposed and has been realized with a good success [13]. This development has permeated to use a charge exchange injection for accumulation of high intense beams of polarized ions in circular accelerators [14].

FEATURES OF SPS

Many versions of the SPS have been developed and optimized for different applications. Cesium admixture enhances negative ion formation in all types of discharges, but the most efficient negative ion production and highest beam quality is attained using an SPS that is optimized for each application. Some basic discharge configurations of SPS are presented in **Figure 1**. Compact SPS (CSPS) such as planotrons (plane magnetron) are seen in (a) and (b). A Penning discharge CSPS is shown in (c). A semiplanotron is shown in (d), and (e) is a hollow cathode SPS using a cold cathode glow discharge in a crossed $E \times B$ field. These CSPS have high plasma density, high emission current density of negative ions (up to 8 A/cm^2), small cathode – emitter gap (1-5 mm) (2) and small extraction aperture in the anode (1). They are very simple and effective, have a high brightness and high pulsed gas efficiency. CSPS are very good for pulsed operation but electrode power density is often too high for DC operation. The opposite situation exists in the Large Volume SPS (LVSPS), presented in **Figure 1**, f, g, h, and first developed in Lawrence Berkeley Laboratory (LBL) [15]. The gap between emitter, 5, and extractor aperture is very large (8-12 cm) and the plasma and gas density must be kept low to prevent negative ion destruction. LVSPS use a hot filament, 7, an RF coil, 9, or microwave discharge and multicusp magnets, 8, for plasma confinement. LVSPS have a

low power density and can be used for DC operation. Emission current density is only about 20 mA/cm^2 and the brightness is not so high. Some versions of LVSPS with emitter (5) were adapted for heavy negative ion production [16]. LVSPS with production of negative ions on the plasma grid surface (anode production on Fig.1g) were adopted for high current (up to 40 A) negative ion beam production for plasma heating [17].

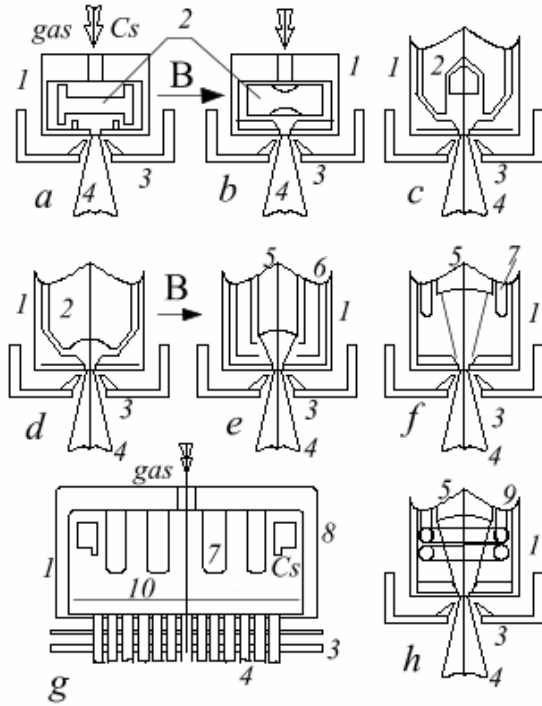


Figure 1. Schematic diagram of the basic versions of SPS: (a) planotron (magnetron) flat cathode; (b) planotron (magnetron) geometrical focusing (cylindrical and spherical); (c) Penning discharge SPS (Dudnikov type SPS); (d) semiplanotron; (e) hollow cathode discharge SPS with independent emitter; (f) large volume SPS with filament discharge and biased emitter; (g) large volume SPS with anode negative ion production; (h) large volume SPS with RF plasma production and emitter. 1- anode(gas discharge chamber); 2- cold cathode-emitter; 3- extractor with magnetic system; 4- ion beam; 5- biased emitter; 6- hollow cathode; 7-filaments; 8- multicusp magnetic wall; 9- RF coil; 10- magnetic filter.

The efficiency of negative ion formation depends very much on the catalytic property of the surface, mainly the work-function. For enhanced negative ion formation in the SPS a mixture of substances with low ionization energy, such as alkaline or alkaline earth elements or compounds, are used. Most efficient is the addition of cesium. Still the surface work-function and catalytic properties of the surface for negative ion formation depends very much on many parameters such as surface-cesium concentration, admixtures of other compounds, such as oxides, halides, nitrides, and surface temperature. Small changes in the surface condition dramatically change the efficiency of

negative ion formation. It is a fine art and some magic to optimize the surface and plasma condition for high efficiency of negative ion formation. This condition is a strong reason for the variation in efficiency of negative ion production although conditions look very similar. Small changes in the surface condition can increase or decrease the intensity of a negative ion beam by large factors. The intensity of H^- beams can have a variation up to 10 times for the same discharge current. A stronger variation can have beam brightness. An efficient ion temperature can have variations from a part of eV to some keV.

A highest brightness for positive ion beams was reached in arc discharge ion sources with a multislit extraction system, developed by Dimov et al. in 1965 and improved with Roslyakov and Davydenko [18]. Review of recent results in this field was presented in [19]. In an arc discharge source we have cooling of plasma ions down to $T_i = 0.2-0.05$ eV by extension of the plasma from a very high density at a point like generator up to a current density $j \sim 1$ A/cm² on the emission surface. This development allowed one to enhance B_n up to 1 A/(mm mrad)² and j/T_i up to 1 A/cm² eV. For a long time, this result was inaccessible for repeating. And for a long time, there was full confidence that this level of brightness was inaccessible for negative ion sources because the emission current density of negative ions was very low.

Brightness dates of negative ion sources for accelerators are collected in recent reviews [9, 20, 21]. From the development of surface plasma sources with cesium catalysis [2,3,4,5,6] the emission current density of negative ions was increased up to $j \sim 8$ A/cm². However, the effective ion temperature recalculated to the emission surface often was quite high also ($\sim 10^3$ eV or more) in the first versions of the SPS and, typically, j/T_i was only $10^{-2}-10^{-3}$ A/cm² eV. The ratio j/T_i has been increased up to 0.1 A/cm² eV in many operating H^- injectors, and up to 0.25 A/cm² eV in improved versions of SPS [22]. For ion sources with volume formation of negative ions the ratio j/T_i is 0.1 A/cm² eV or less, because the emission current density is low [9, 20]. In SPS with cusp plasma generators, and with big gap between the emission surface of the converter and the emission hole, the typical j/T_i is 0.01 A/cm² eV [20].

The level of $j/T_i = 1$ A/cm² eV can be reached in surface plasma sources with high current density after special optimization, in noiseless regimes of discharge and beam formation-transportation. The important aspects of high brightness beam production have been described and discussed in References [5] and [22, 25, 26, 29]. Here, we will present some comments on these results.

For high brightness beam production is necessary to have a high density of cold ions: for $j = e n v/4 \sim 1$ A/cm² and $T_i < 1$ eV it is necessary to have $n > 2 \cdot 10^{13}$ cm⁻³ on the emission surface. In SPS, it is quite easy to have an emission current density up to 5 A/cm² by using geometrical focusing of negative ions emitted from the cathode surface and accelerated by the discharge voltage. But the ion energy in this case is $e U_d = 100$ V, and the effective ion temperature is $T_i \sim 10$ eV. The necessary parameters of ion flow can be produced by conversion of these accelerated ions into cold negative ions by resonant charge exchange. The cross-section for this process is 10^{-14} cm², and for an effective concentration of cold ions near the emission surface, a cold atom density $n_H \geq 10^{15}$ cm⁻³ is necessary. The emission of negative ions from the walls of the emission slit, catalyzed by a cesium film on the surface (anode surface-plasma generation), and their charge-exchange will also play an important role in the production of a high density of cold

negative ions. Collisions with the walls must be the important mechanism for cooling of atoms, and its efficiency will be higher for a smaller cell. The effective extraction of negative ions from discharges with too high gas density is possible if the extraction hole is small ($d \sim 1 \text{ mm}$) and the thickness of the gas target Knd for negative ion destruction after extraction is low enough. This is important also for prevention of voltage breakdown in the extraction gap. The perveance and intensity of the beam can be increased by using slit extraction geometry, with length of slit l . By using these distinctive features, it is possible to guarantee the generation of a high density flow of cold negative ions, required for high brightness beam production. However, the effective ion temperature can be increased very much by aberrations in the extraction system, and by fast fluctuations of electric fields.

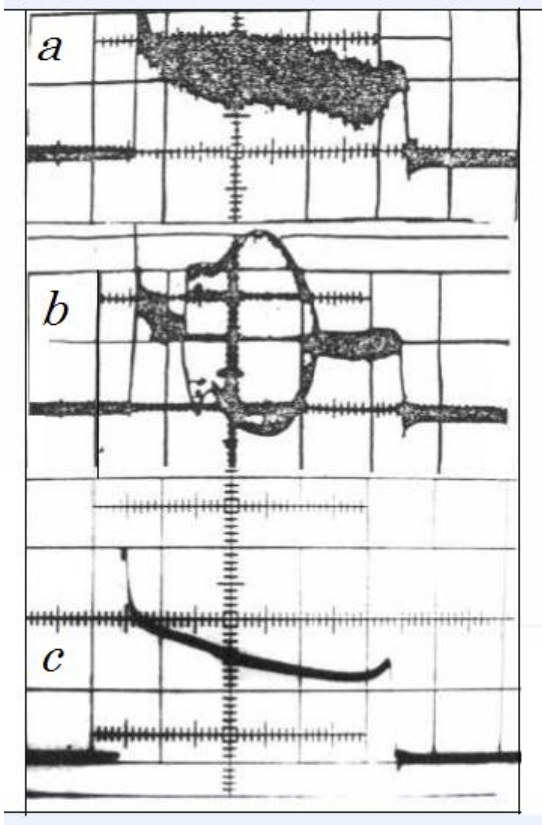


Figure 2. . The examples of discharge voltages for different conditions in SPS. (a) A discharge with noise; (b) a discharge with RF generation; (c) noiseless discharge. Vertical scale is 100 V/div; Horizontal scale is 0.2 ms/div.

For low aberration beam formation in magnetic field the slit extraction system is very suitable. This property of slit extractors has been used for the measurement of the transverse temperature of positive [18] and negative ions [2226], with good preservation of the low ion temperature along the slit. In the perpendicular direction, it is more difficult to eliminate aberrations, but this problem is the same as in extractors with

circular aperture. The decreasing of the emission slit dimension along the magnetic field, d , (and increasing of effective wall thickness h) is very effective for suppression of coextracted electron flow [3, 45]. Minimizing of electron current I_e is very important for maintaining high brightness, and for breakdown preventing. The optimization of the configuration of the extraction electrodes, and operating at the proper emission current density, for a given extraction voltage, help to minimize the aberrations and effective ion

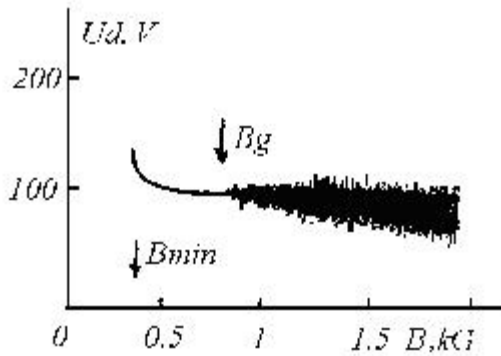


Figure 3. The discharge voltage and level of noise vs. magnetic field in SPS with Penning discharge.

temperature in the small size direction. To maintain the brightness, it is very important to have a noiseless discharge and noiseless beam formation-transportation. Examples of discharge voltages with difference levels of noise and RF generation are presented in Figure 2. The level of noise can be very high, with broad frequency band, as (a); the coherent RF voltages (18-20 MHz) can be generated in discharge, as (b); but it is possible to have noiseless discharge, as (c). The typical dependence of the discharge voltage and level of noise on the magnetic field B is shown in Figure 3. The low pressure high current discharge can be ignited only if $B > B_{min}$. It is possible to have a noiseless discharge in the region between B_{min} and B_g . The width of this noiseless region depends on the gas density as shown in Figure 4, and on the discharge cell size D . It is possible to have a noiseless regime only if the gas density is higher than the threshold level n_c . For increased cell size D , the minimum magnetic field B_{min} can be lower, and the threshold density n_c can be lower also. The decreasing of discharge voltage U_d is useful for noiseless discharge creating because help to decrease the critical magnetic field and decrease critical gas density.

The properties of SPS discharges can be explained by the dependence of the transverse electron conductivity C in crossed ExB fields and the scattering frequency $\nu = 1/\tau$. The transverse current density $j_e = C E = e n_e \mu E$.

The mobility μ is:

$$\mu = e\tau/m (1 + \omega^2 \tau^2) = e\nu/m (\nu^2 + \omega^2), \quad (2)$$

where ω is Larmor frequency. The dependence of mobility on effective scattering frequency is shown on

. It has a maximum when $\nu \sim \omega$. The classical scattering frequency ν_c depends on the gas and plasma density n_g , scattering cross-section σ_s , and electron velocity v_e . The excitation of noise will increase the effective scattering frequency of electrons. The noise will increase conductivity if $\nu_c < \omega$, and will decrease transverse conductivity if $\nu_c \geq \omega$. In this last case the excitation of noise must therefore be impossible, because it would lead to an increase in the discharge voltage. For a noiseless discharge one needs to have:

$$\nu_c = n_g \sigma_s v_e > eB/mc \quad (3)$$

or for effective gas density (including plasma)

$$n_g \geq eB/mc \sigma_s v_e \quad (4)$$

If the classical scattering frequency is lower than ω , the excitation of noise is “profitable” because the conductivity of the discharge has increased. The Larmor radius R of electron in the minimal magnetic field B_{min} must be less than transverse size of cell D :

$$R = pc/eB < kD, \quad (5)$$

where k is an empirical coefficient $0.1—0.5$.

For generation of highly concentrated negative ion flow, one needs to use gas discharge cells with the smallest size D of mm scale. For discharge voltage $U_d = 100 V$ (with cesium catalyst) the minimum magnetic field $B_{min} \sim 0.05 T$, and ν_c must be more than $10 GHz$. The corresponding effective gas density (and plasma density) must be quite high ($\sim 10^{15} cm^{-3}$). Having a noiseless discharge therefore limits the dimension of the extractor aperture d to the mm scale due to the increased gas density. The beam intensity can be increased while keeping a high brightness by using slit extractor geometry.

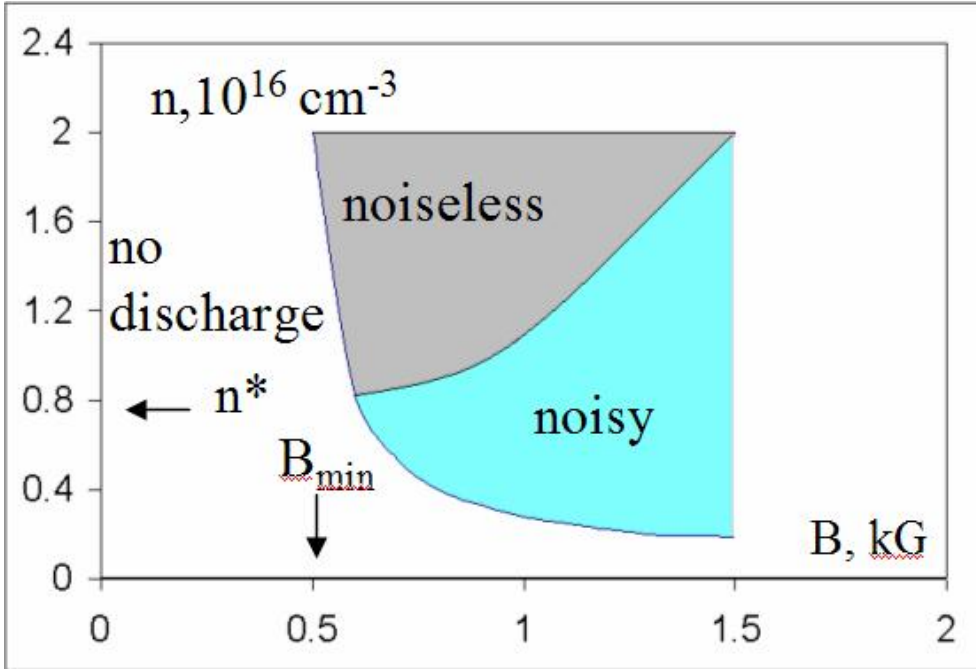


Figure 4. A schematic diagram of discharge noise on plane: magnetic field, gas density.

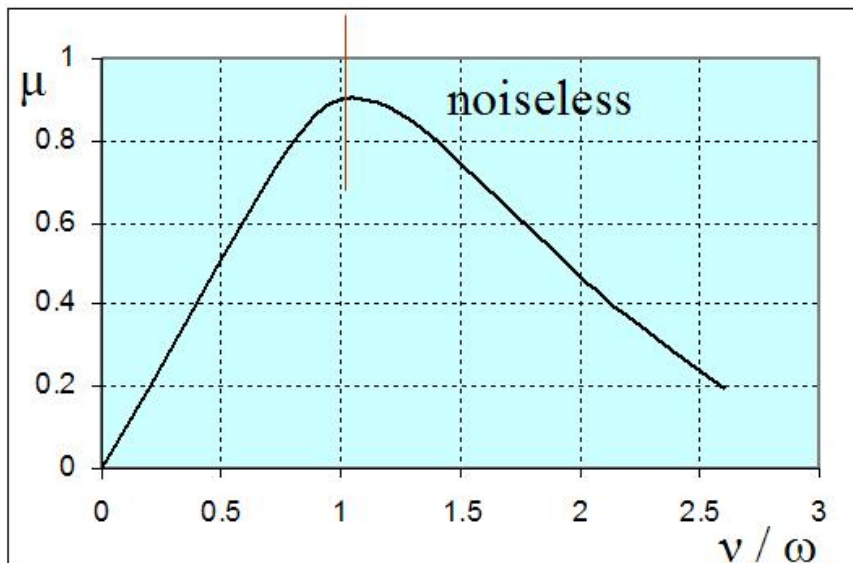


Figure 5. The dependence of mobility on effective scattering frequency.

It is easier to have stable operation with not very high beam parameters such as intensity $I \sim 30-50 \text{ mA}$, emission current density $J \sim 0.5-1 \text{ A/cm}^2$, transverse ion temperature $T_i \sim 5-10 \text{ eV}$. Present experience permits better optimization for longtime stable production of high-brightness high-intensity beams of negative ions ($I \sim 0.1-0.15 \text{ A}$, $B \sim J/T_i > 1 \text{ A/cm}^2 \text{ eV}$, lifetime $N > 10^8-10^9 \text{ pulses}$). Highest brightness could be realized only with noiseless

operation. The level of discharge noise (hash) is depended of many parameters. For stable discharge a surface properties should be in the stable conditions and frequency of electron scattering by plasma particles should be higher than Larmor frequency. A discharge noise could be suppressed by decrease of magnetic field as shown in *Figure 3* and by increase a gas or Cs density. Examples of discharge voltages with a different level of noise are shown in *Figure 2*.

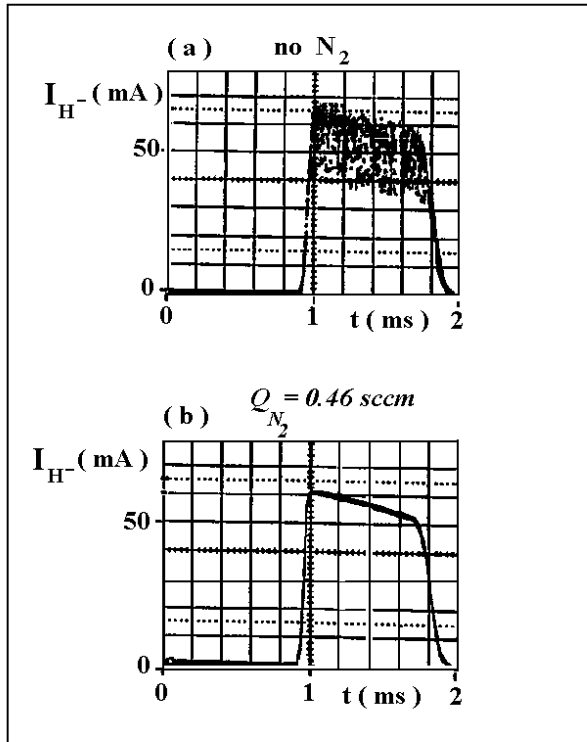


Figure 6. Suppression of discharge noise by adding a small admixture of nitrogen in the LANL Penning CSPS [20].

Admixture of heavy gas could be useful for noise suppression, but it increased a sputtering. Example of noise suppression by admixture of heavy gas neutragen, demonstrated in Los Alamos National Laboratory is shown in *Figure 6* [20]. A transition from the noise discharge (a) to noiseless one (c) increases a beam brightness at order of magnitude.

NEGATIVE ION SOURCES FOR ACELERATORS

The first versions of the Surface-Plasma Sources (SPS) developed for charge-exchange injection of protons have an operating intensity $I \sim 50$ mA with pulse lengths of 0.05-1 msec, noisy discharges and a repetition rate up to 50 Hz [6-11]. H^- beam parameters of these SPS were sufficient for normal operation of large proton accelerator complexes during the past 25 years without significant modernization of ion sources.

Now, new accelerator projects need an increase of the ion beam intensity and brightness. Some upgrading of existing SPS could achieve the necessary increase of intensity, duty factor and beam quality without degradation of reliability and availability of the achieved satisfaction level.

Planotron (plane magnetron)

Planotron (plane magnetron) shown in **Figure 1 (a), (b)** has a longest experience in testing and operation in accelerator complexes. The first version of planatron is shown in **Figure 7**. Main parts of this design were welded by spot welding from Stainless Steel and Molybdenum or Tantalum foils. But this very simple design was able to generate up to

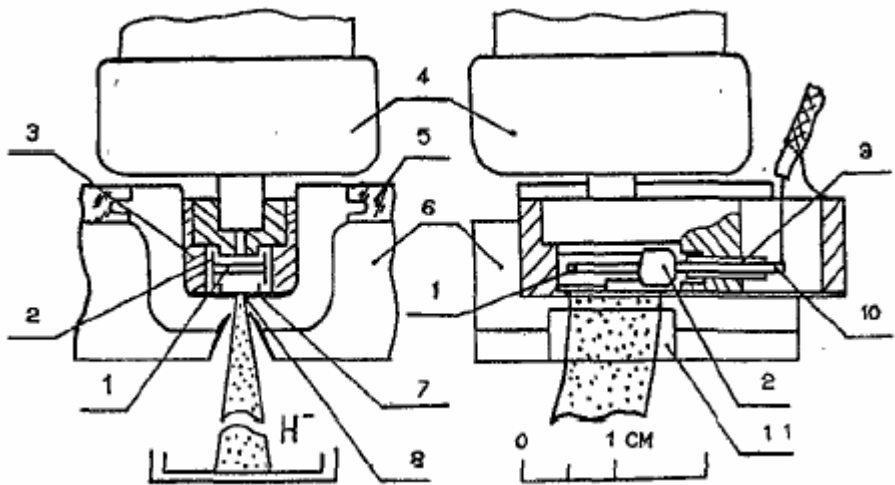


Figure 7. First version of planotron (plane magnetron).

(1) cathode (central plate); (2) cathode (side shields); (3) anode (body of the discharge chamber); (4) pulsed gas valve; (5) high voltage insulators; (6) magnet poles; (7) collar"plate; (8) emission slit; (9) cathode insulators; (10) cathode holders; (11) extractor.

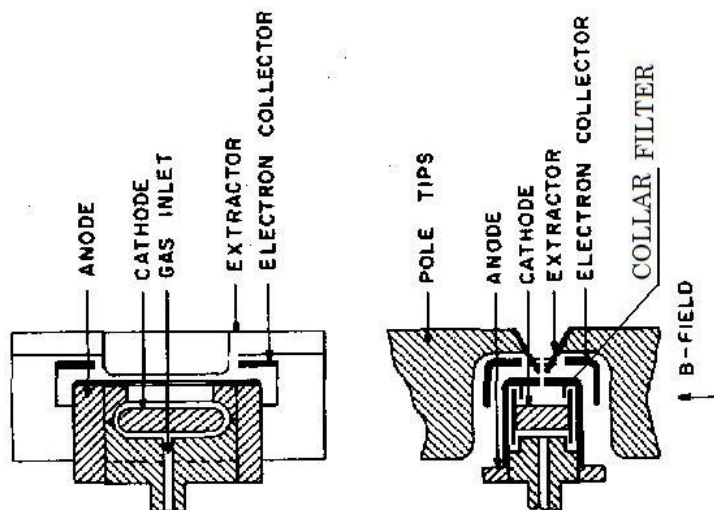


Figure 8. Upgraded version of planotron with emission current density up to 3.7 A/cm^2 .

230 mA of H^- with current density up to 1.5 A/cm^2 in 1 ms pulses with repetition up to 10 Hz. Main features of planotron are small gap between cathode and anode and emission slit perpendicular to magnetic field lines. The upgraded version of planotron with capability to current density up to 3.7 A/cm^2 is shown in **Figure 8**. This version has a “thick” cathode and more robust electrode holder and can reliably operate with smaller gaps between electrodes. Energy spectra of H^- from planotron are shown in **Figure 9**. The ion spectra from a planotron usually have two peaks separated by a valley. The location of the first peak coincides with the accuracy of

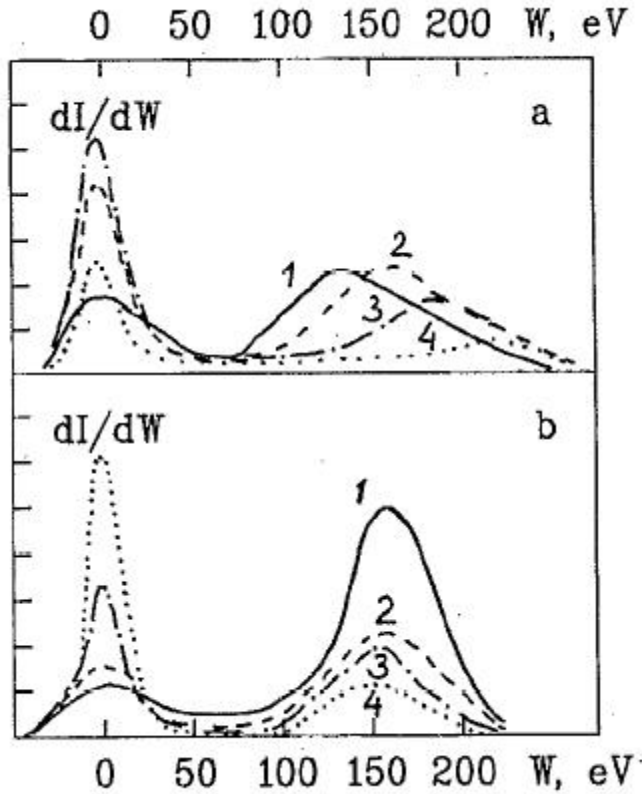


Figure 9 Energy spectra of H^- from planotron.

the measurement (~ 10 eV) with the energy eU_{ex} imparted to the negative ions by the extraction voltage. The ion energy of the second peak is higher than that of the first peak by an amount close to eU_d . The oscillograms in the upper part of **Figure 9** illustrate the change in the spectra, as a result of increasing the discharge voltage U_d from 120 V (1) to 210 V (4) by reducing the cesium supply. The oscillograms (1-4) in the lower part of **Figure 9** illustrated how the spectra vary as a result of increasing the hydrogen supply to the discharge chamber. When the hydrogen supply is the lowest and the cesium supply is optimum, a large fraction of ions from planotron discharges will be accelerated by the full discharge voltage, but the amplitude of the peak with the higher energy will rapidly decrease with increasing hydrogen supply and the amplitude of the first peak will increase. Gas injection optimization can be used for transformation of fast primary H^- from cathode to the cold H^- for high brightness beam formation.

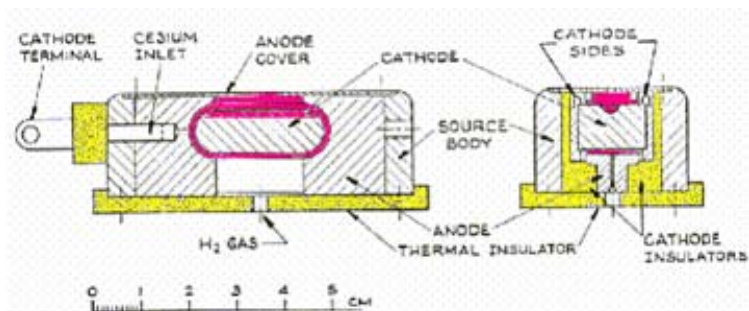


Figure 10. Design of Fermilab magnetron.

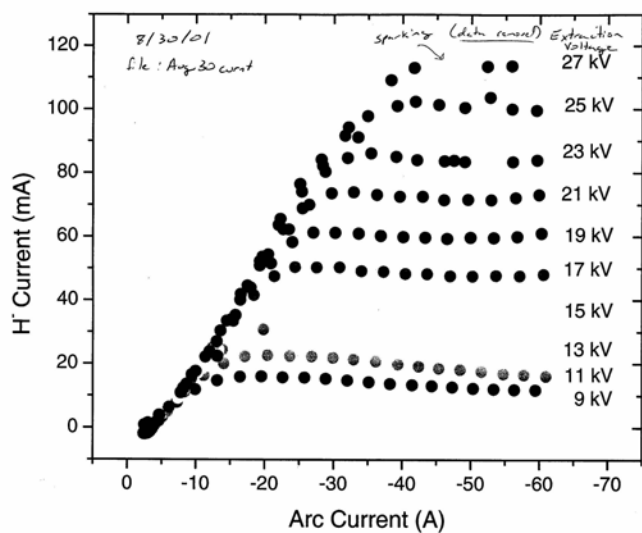


Figure 11. Dependence of H- beam current after analyzer magnet on discharge current for different extraction voltages for Fermilab magnetron.

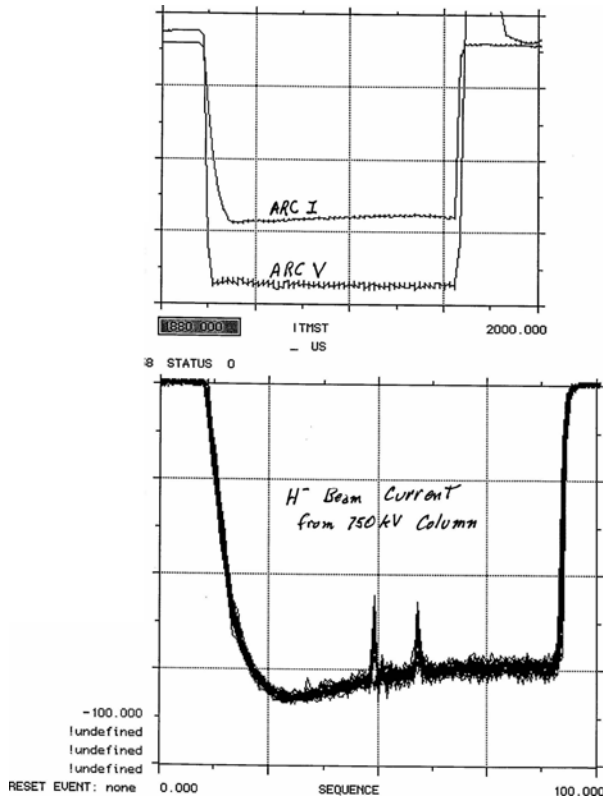


Figure 12. Oscilloscope tracks of discharge and H⁻ pulses in magnetron.

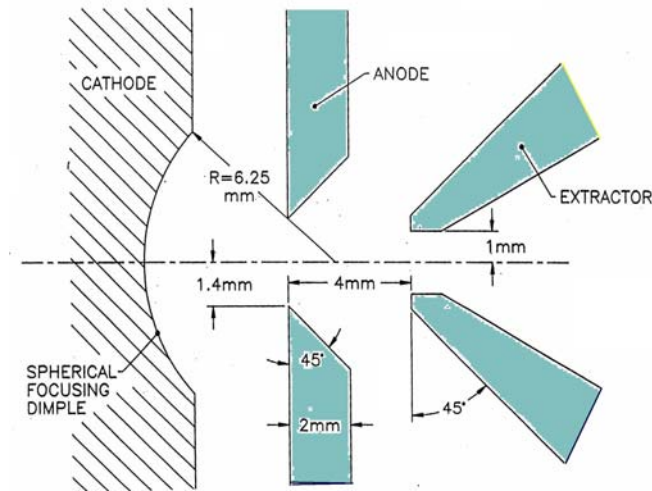


Figure 13. BNL version of magnetron. (Discharge gap and extractor).

The Fermilab Magnetron SPS, designed by C. Schmidt is shown in **Figure 10**. It has been operational in Tevatron accelerator complex since 1978 [17]. Efficiency of H⁻ generation was improved by cylindrical geometrical focusing, developed in Novosibirsk INP [38]. The peak current of the H⁻ ion beam at the exit of the 750 keV accelerator

column is $I_b=65\text{ mA}$ with an extraction voltage $U_{ex}=20\text{ kV}$, and $I_b\sim 70\text{ mA}$ with $U_{ex}=25\text{ kV}$ with a beam pulse length $T=0.075\text{ msec}$ at 15 Hz . The pulse length could be increased with a new arc discharge pulser and adjusted parameters. It is useful for stable operation to have a discharge power supply as a current source with a high impedance ($Z=5\text{-}10\text{ Ohm}$, now $Z=1\text{ Ohm}$) and corresponding higher voltage. After optimization of the discharge electrode configuration the intensity was increased above $I_b=0.1\text{ A}$ without increasing the discharge power. Dependence of H- beam current after analyzer magnet on discharge current for different extraction voltages is shown in **Figure 11**. In production mode discharge has some noise as shown in discharge pulses in **Figure 12**. This noise is reason of any increase of beam emittance in magnetrons. Gas delivery optimization should allow a longer pulse and higher intensity without an increase of the gas loading. Fermilab magnetron was adapted in Argonne Intense Pulsed Neutron Source and in BNL. Later in BNL magnetron was adopted a spherical geometrical focusing and circular emission aperture for injection in RFQ. A schematic of this version of magnetron is shown in **Figure 13**. A dependence of H- current on extraction voltage is shown in **Figure 14**. This dependence is very strong, because beam intensity is space charge limited. This design is very good for production of 100 mA pulses with df up to 1% (discharge power 30 Wt). With low voltage discharge ($U_d=100\text{ - }150\text{ V}$) and good cesium optimization electrode sputtering by discharge is very low and don't limit operation up to 9 months. More significant is a cathode sputtering by back accelerated positive ion, because a simple two electrode extraction system don't prevent transportation of positive ion from the beam to extractor gap. But this very compact and simple version of magnetron was tested for many months continue operations in many accelerators with high voltage injectors and with RFQ.

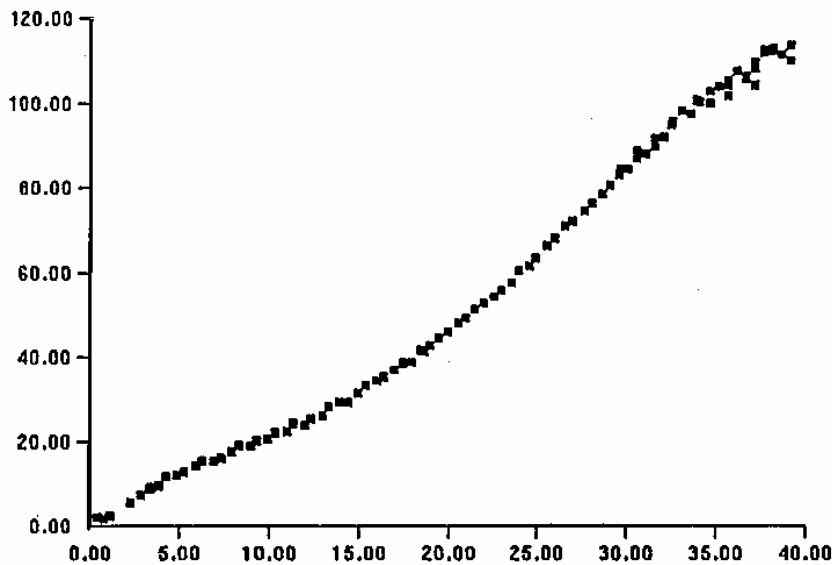


Figure 14. Dependence of H- beam current on extraction voltage in BNL magnetron.

A possibility of magnetron upgrading for longer duty factor is discussed in Ref [24]. An optimized extraction system with a suppression electrode should improve the beam intensity, beam quality and beam space-charge neutralization with a low gas pressure. A

suppression of a back accelerating of the positive ion should suppress cathode and anode sputtering by accelerated positive ions - a main reason for the shorting of ion source lifetime. Improved cathode and anode cooling is necessary for increased discharge pulse length and intensity.

CSPS with a Penning discharge.

CSPS with a Penning discharge was produced from planotron by removing of the central cathode plate. A fundamental difference between the magnetron- planotron and CSPS with a Penning discharge is that the H^- ions from the magnetron cathode production surface have line-of-sight trajectory to the emission surface, while H^- produced on the Penning cathode must undergo the charge-exchange process on atomic hydrogen [5] to reach emission. Anode SPG is important process of H^- production in these SPS. Energy spectrum of H^- from Penning SPS is shown in **Figure 15**. It has only one sharp anode pick. In this regard, emittance measurement has shown highest beam brightness for the Penning SPS. A first “robust” version of Penning CSPS for accelerators with a high H^- beam brightness was described in ref. [5].

Lot of work for development of this version of CSPS was done in Los Alamos National Laboratory and in LBL [20, 22]. A version of this Dudnikov type SPS with the Penning discharge, well reproduced in Los Alamos is shown in **Figure 16**. This version of CSPS was adopted for using in ISIS spallation neutron sources in Rutherford Appleton Laboratory [31]. A schematic of ISIS Penning source is shown in **Figure 17**. Describing of this source operation is presented in references [31,32]. Upgrading for higher parameters is discussed in ref. [32].

The SPS H^- sources are in use at the majority of operating charge-exchange based synchrotron accelerators. Table 2 shows a summary of representative results on the magnetron and Penning H^- SPS sources. All sources use a slit emission-extraction system $0.5 \times 10 \text{ mm}^2$ except the BNL magnetron that uses a 2.8mm diameter emission aperture. The LANL 1X Penning and ISIS Penning have essentially the same discharge chamber dimensions as in the first version of INP Dudnikov type SPS. The RAL Penning source that is in use at the ISIS facility delivered 35 mA after pre-accelerator with $df \sim 2.5\%$,

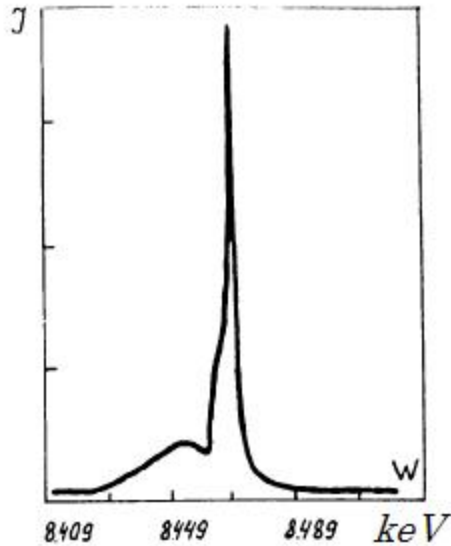


Figure 15. Energy spectrum of H^- from Penning discharge SPS.

during period up to 50 days. This version of SPS has weak cooling because it was optimized for low df operation. A thin plasma plate has low thermo conductivity and can be overheated. This ion source is under development at RAL for possible ESS application [32]. The development goals are 70 mA H^- current at short-pulse df of 1.2 ms, 50 Hz, and 70 mA H^- current at long pulse df of 2.5 ms, 50/3 Hz. Design emittance (1 rms, normalized) is < 0.3 (π mm mrad) with lifetime of > 20 days.

Penning SPS for higher average current was build and tested in the BINP in 1976 [25]. **Figure 18** shows a schematic of this CSPS. Operation with beam current above 100 mA after analyzer magnet in pulses 0.25 ms, repetition $f=100$ Hz has been tested during 300 hours ($df = 2.5\%$). Operation of this SPS with forced cooling was tested up to repetition rate of 400Hz, 100 mA, df up to 10%. Distinctive features of this Penning SPS are little increased discharge cell, massive plasma plate with a deep magnetic filter and with forced air or water cooling of cathode and anode. Fast gas valve (10) can inject gas during 0.1 ms with repetition up to 800Hz. Noiseless discharge is important for high brightness beam production.

TABLE 1. Summary of magnetron and Penning H^- SPS.

Source	$I(H^-)$ (mA)	Pd (kW)	P_{eff} (mA/kW)	e/H^-	df (%)
BNL-magnetron	100	2.2	45	1	0.7
Fermilab-magnetron	80	5.1	15.8	2	0.13
DESY-magnetron	60	6.6	9.1	2	0.12
ISIS-Penning	35	2.8	12.5	2.8	2.5
LANL-1X Penning	108	4.8	22.5	1.6	0.5
LANL-1X Penning	160	18	8.9	2.2	0.5
LANL-4X Penning	250	18.3	13.7	2.2	0.5
BINP-Penning	150	10	15	1	2.5(10)
BINP-semiplanotron	120	2	60	1	1.25

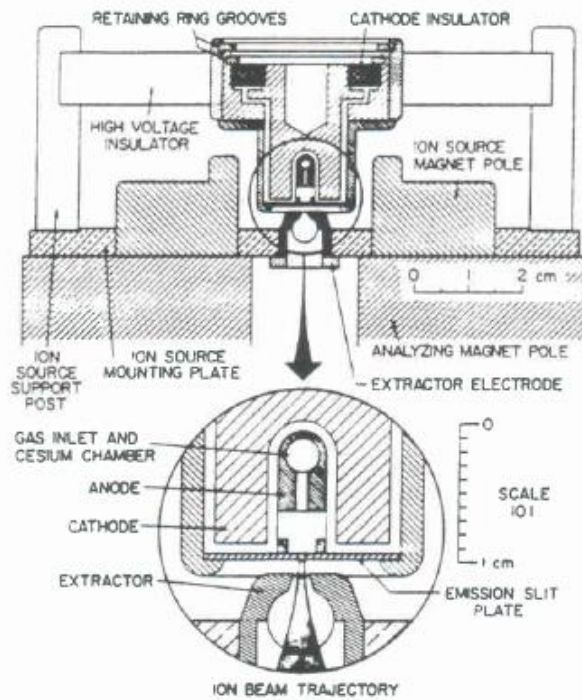


Figure 16. Schematic of Los Alamos version of SPS with Penning discharge.

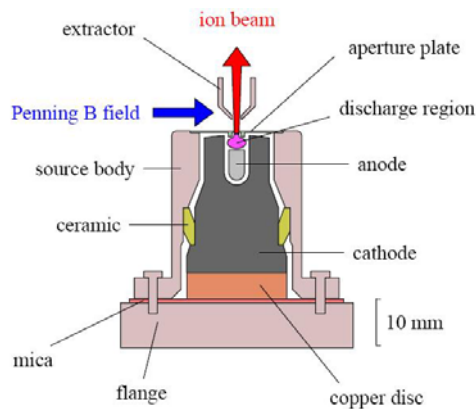


Figure 17. Schematic of ISIS version of Penning discharge SPS [].

A schematic of H- beam formation with bending one dimension focusing magnet and system for emittance detection are shown in **Figure 19**. Oscillogram of this CSPS operation with a repetition of 100Hz is shown in **Figure 20**.

In reports [33] is predicted using a discharge scaling laws and the 250 mA results that 4X Penning H- SPS, scaled from an original 1X Dudnikov Type SPS [522] with a

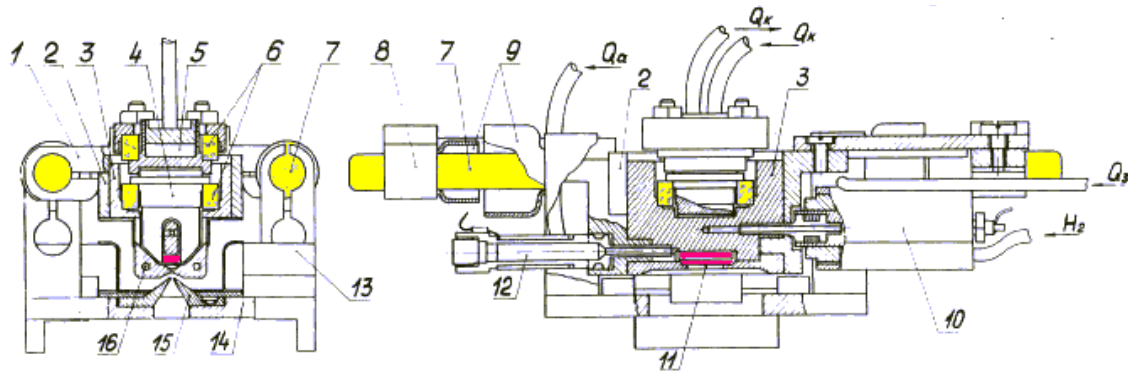


Figure 18. Compact Surface-Plasma source with Penning discharge (Dudnikov type source). 1- support; 2- gas discharge chamber; 3-anode insert; 3- cathode; 5-cathode cooler; 6- cathode insulator; 7- high- voltage insulator; 8-support; 9-insulator shielding; 10-fast gas valve; 11-emission slit; 12-cesium oven; 13-magnetic pole; 14-base plate; 15-extractor; 16-anode cooling

slit emitter would be capable of producing > 100 mA, low emittance H- beam in a 5% df range (1 ms, 50Hz).

Authors are using assumption that primary H- ions produced in the cesiated cathodes surfaces and are transformed into cold, extractable H- ions by resonant charge exchange of fast primary H- with cold H atoms inside collar area. This concept was developed for original 1X version of Dudnikov type source [5], having a small distance between cathodes surface $\sim 4-5$ mm and used in RAL [31]. In discharges with increased distance between cathodes surface and emission aperture, H- ion from cathodes surfaces can't reach emission slit area without destruction. In this case only surface plasma generation of H- on the plasma electrode (anode SPG) around emission aperture is important. Previous experiments [34] are demonstrated, that this anode SPG is very efficient. In the previous experiments for plasma generation was used discharge with a cold molybdenum cathode in hydrogen with cesium admixture. Admixture of cesium decrease a work function of cathode and anode, increase a secondary emission of electrons and negative ions, decrease discharge voltage and sputtering. But for stability of optimal cesium film on cathodes is important to keep optimal temperature of surface. For high duty factor it can be difficult. But in discussed situation it is critical optimal cesium coverage only on the anode surface around the emission aperture, where a power density is not too high and can be preserved in optimal conditions easier. For plasma generation it is possible to use discharge with other cathode materials with a low work function, as oxide cathode or lanthanum hex boride LaB6. For efficient anode SPG it is necessary to generate a flux of H atoms with energies above threshold for H- emission, equal of difference between work function and electron affinity $\phi-A=1.6-0.75\sim 1$ eV.

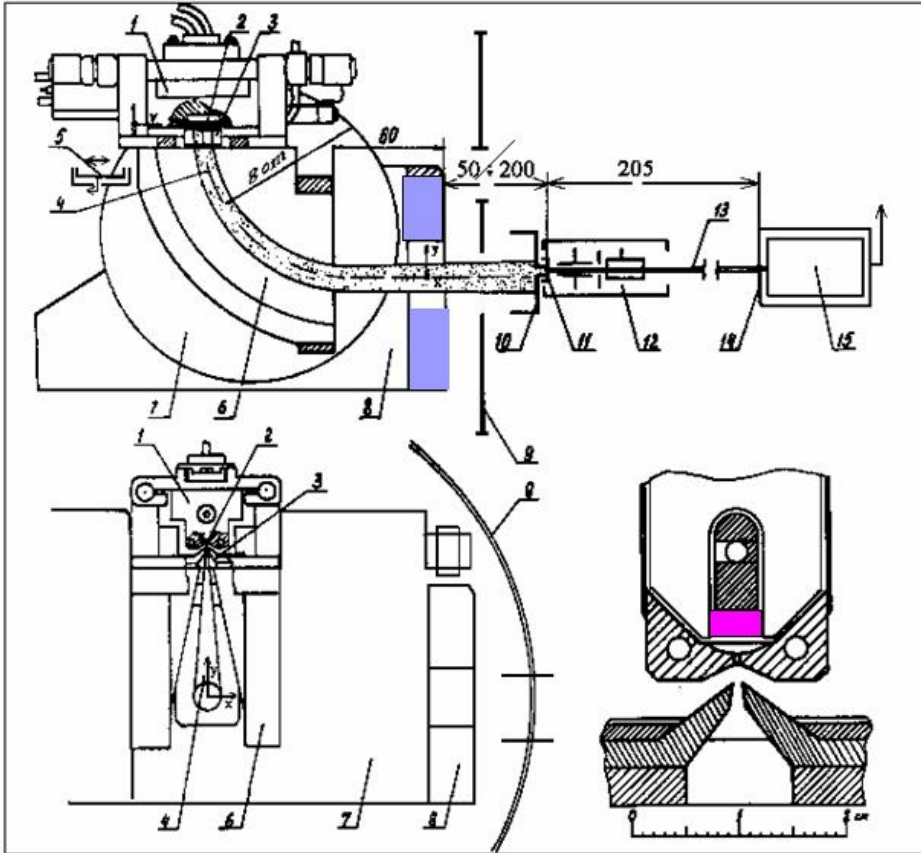


Figure 19. Schematic of beam formation and diagnostics with a bending magnet.

A plasma generation with LaB6 cathode in the Dudnikov type source was tested successfully in several works [343536]. A conclusion from these experiments, that H- ions are generated by volume processes was not correct. In these discharges without cesium an anode SPG was a dominant process of H- production. Of course without cesium an efficiency of anode SPG is not too high as with cesium catalysis. Efficiency of H- production was increase in [2337] by adding of cesium. But this mode of operation was less efficient, than cathode SPG in planotron with geometrical focusing. But sources with anode SPG have better scaling to higher duty factor. In sources with large sizes should be better condition for plasma (and fast atoms) generation. A cesium concentration and conditions for anode SPG should be optimized on the anode surface only. Efficiency of

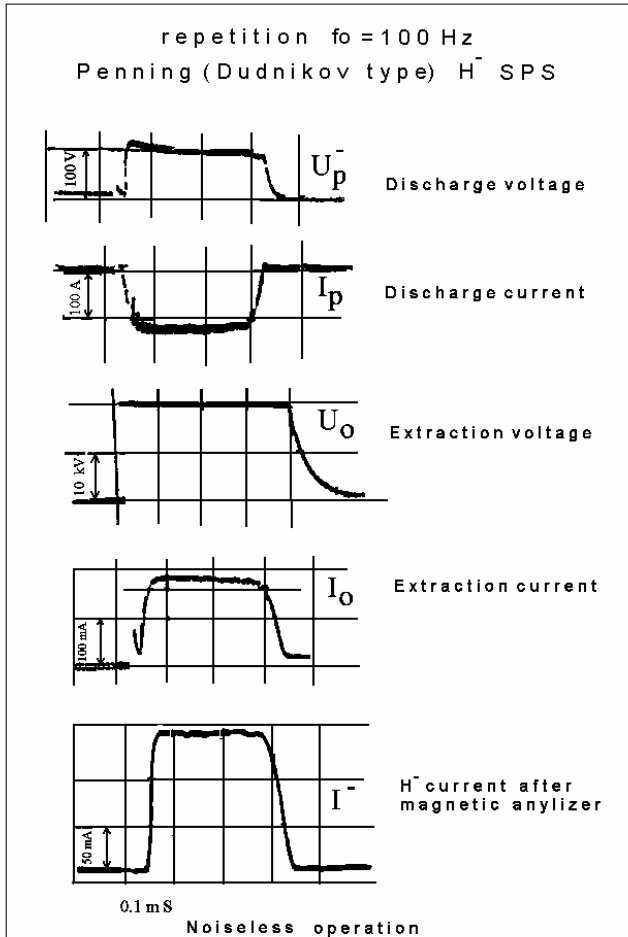


Figure 20. Oscillogramms of 100 Hz operation of Penning CSPS with forced cooling

H^- generation can be increased by correct shape of plasma electrode with emission aperture [25] and controllable bias voltage relative anode potential. Other possibility of fast atoms generation is using of RF discharge, as in DESY SPS [12] and in SNS SPS [20]. As was scaled from [33] in 4X Penning SPS is enough use ~ 8 kW of discharge power for production of 100 mA of H^- with slit 2.8×11 mm². Using a high temperature cathode near the emission aperture is complicated preservation of optimal cesium coverage on the plasma electrode around emission slit. It is better to have thermo emitter in any distance from the aperture and use plasma drift for delivery plasma and fast atoms to the plasma electrode. The use of RF discharge for fast atom generation is preferable, because is no heat generation between pulses.

Semiplanotron CSPS.

An H^- beam with high characteristics was obtained from the semiplanotron SPS. The schematic view of semiplanotron is presented in **Figure 21**. It has a very simple

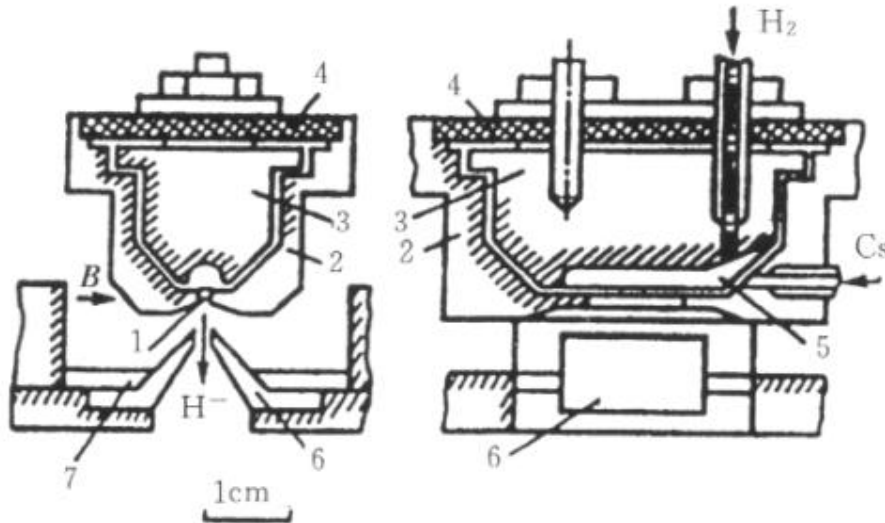


Figure 21. Schematic of semiplanotron SPS. 1- emission aperture; 2- anode; 3- cathode; 4- cathode insulator; 5- discharge channel; 6- extractor; 7- magnet with magnetic insertions.

construction and very small discharge volume - only a semi cylindrical groove on the cathode with the depth $t = 1-3 \text{ mm}$. The discharge is localized mainly near the emission slit with size $d \times l = 0.5 \times 10 \text{ mm}^2$. The discharge in crossed ExB fields is supported between the cathode (3) and the anode (2) in narrow (2-3 mm) semi-cylindrical discharge channel (5), opposite to the emission aperture (1). The discharge is ignited in a deeper groove in the right end of the cathode where working gas and cesium are injected. Plasma drifts in the crossed fields from the right to the left. Electrons oscillate along the magnetic field between the walls of a semi-cylindrical discharge channel, and positive ions bombard its surface, initiating emission of the sputtered and reflected particles. Part of these particles leaves the surface in the form of negative ions. The probability of particles escaping as negative ions increases essentially at the reduction of surface work function due to adsorption of cesium or other substances with low ionization potential.

The slit configuration, the wall thickness h , angle width of slit θ has been changed for optimization of efficiency, of brightness, and of electrons suppression. Negative ions are accelerated by a potential difference between surface and plasma and are focused on the emission aperture due to the cylindrical form of the emitter. During the moving through the plasma part of ions loses electrons in collisions with plasma particles and converts in fast neutrals, as shown in the planotron's energy spectra in **Figure 9**. Part of fast negative ions transfers electron to cold atoms, transforming to cold negative ions. This charge-exchange cooling of negative ions increases beam brightness. Shielding of an emission aperture by equi-potential groove (collar) and a strong transverse magnetic field form the magnetic filter, suppressing plasma diffusion to the emission aperture and extraction of accompanying electrons. The walls of equi-potential cavity are bombarded by fast ions and atoms from the cathode and by less energetic (with energy 5-10 eV) particles from the discharge.

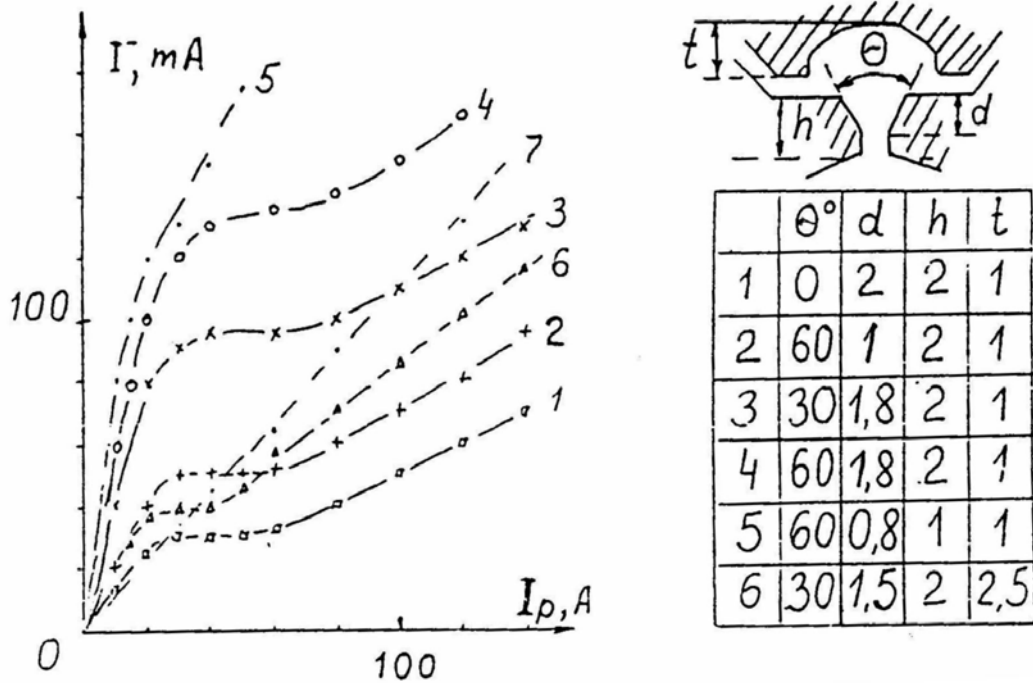


Figure 22. Dependence of H^- current on the discharge current at different geometries of discharge channel and magnetic filter in semiplanotrons. Dependence (7) is obtained in SPS with Penning discharge.

This bombardment causes emission of negative ions from the anode surface around the emission aperture (anode SPG). Low density of electrons in this area and low electron temperature promote survival and effective extraction of negative ions from this area. Emission characteristics of semiplanotron at various configurations of the discharge channel and the magnetic filter are shown in **Figure 22**. Dependences of the intensity of H^- ion beam on the discharge current have the N-shaped form with three sections: linear growth at small discharge currents, saturation or a falling section at medium currents, and linear, but slow growth at the high currents. Linear dependence (7) is obtained in SPS with Penning discharge. At small discharge currents most of extracted NI is provided by SPG on the cathode. In this section the efficiency of SPG is the highest (up to 6 mA on 1 A of discharge current at discharge voltage of 100 V, up to 60 mA per kW). With the increase in discharge current the flow of NI from the cathode is attenuated by destructions in plasma, and less effective anode SPG can not compensate this attenuation that forms a falling section. At the high discharge currents, linear growth of NI current is provided by anode SPG. Emission of positive ions is much less than the emission of NI; the contribution of volume generation of NI is relatively low. Anode SPG provides linear dependence of negative ion current on discharge current in the Penning SPS shown under number (7). The current of accompanying electrons in these measurements was less than the negative ion current in normal magnetic fields $B \sim 1$ kG. In weak fields ($B \sim 0.1$ kG),

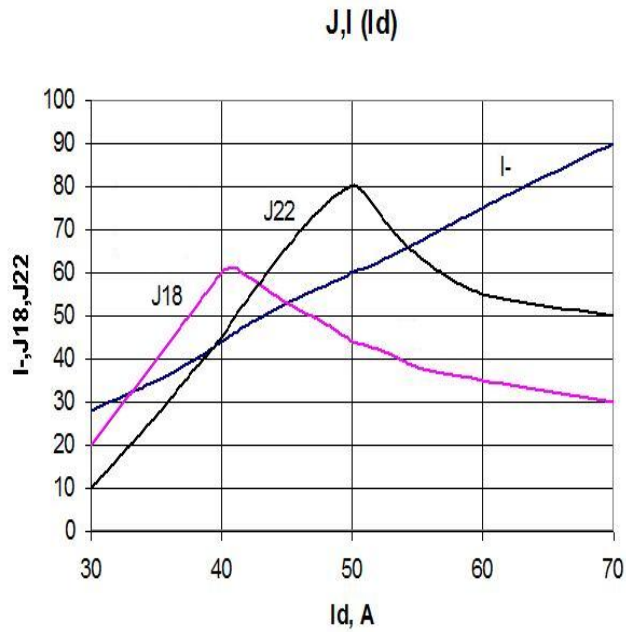


Figure 23. Dependence of H- current and pick current density on discharge current for extraction voltage 18 and 22 kV.

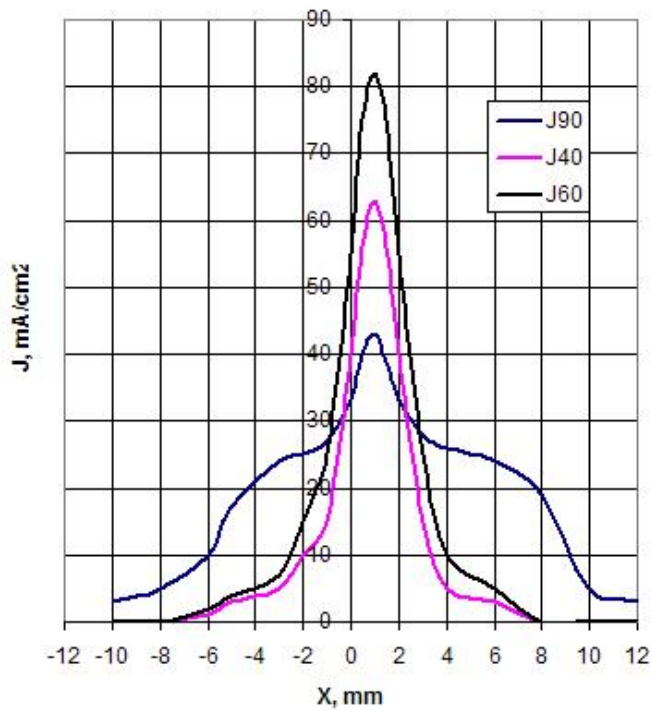


Figure 24. Current density distribution for different relation extraction voltage/current density.

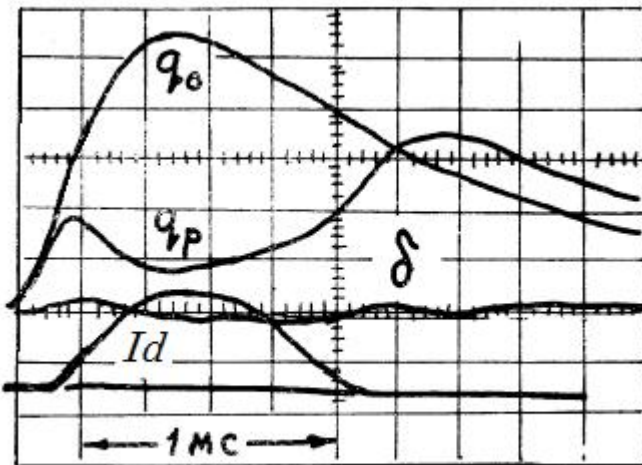


Figure 25. Oscillograms of gas suppression by discharge in compact SPS.

q_0 - Gas flux without discharge; q_p - gas flux with discharge; δ - level of noise and cross talks; I_d - discharge current.

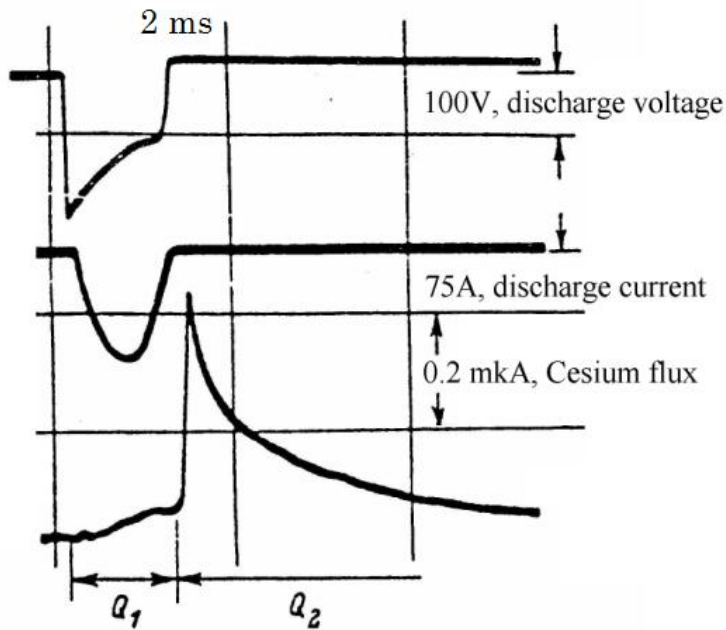


Figure 26. Oscillograms of cesium flux suppression by discharge in compact SPS.

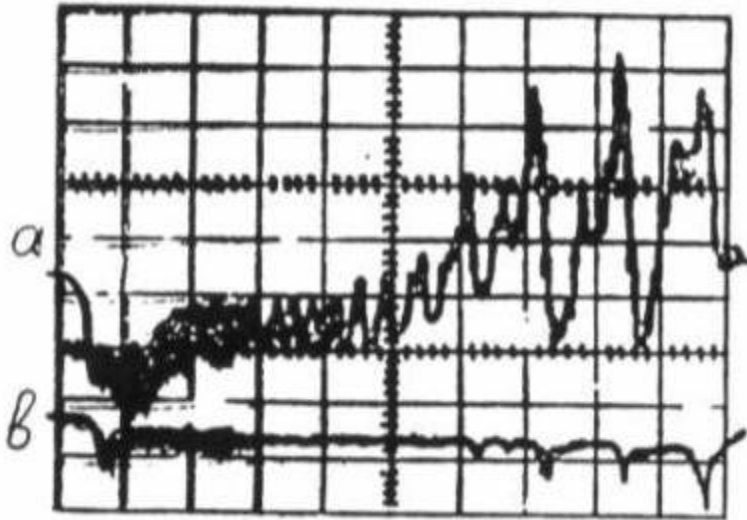


Figure 27. H- beam instability developments with secondary emission of electrons from collector. a- beam collector signal; b- signal from side electron collector.

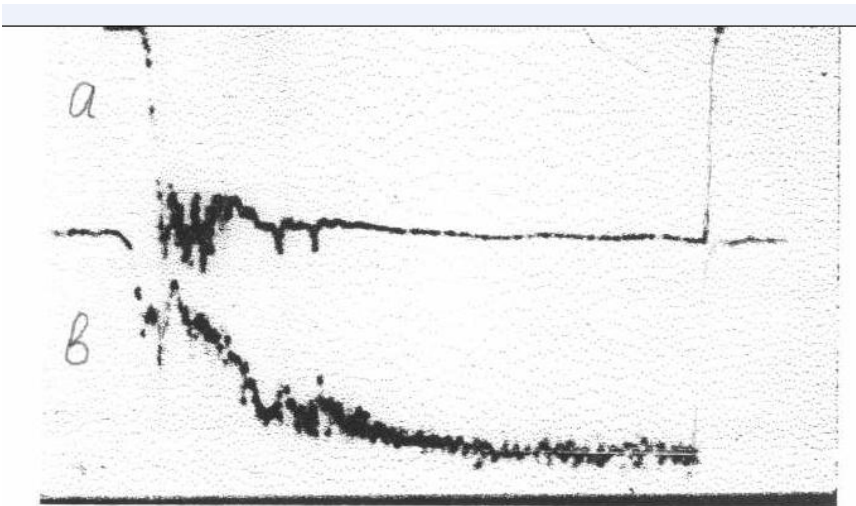


Figure 28. Fluctuation of H- beam current density with noiseless beam current. a- collector current; b- current from small collector (local current density).

the electron current could be 10-20 times greater than the negative ion current. In semiplanotron SPG of negative ions is realized most effectively, For only 20 A discharge current at 100V, the pulsed beam current was 100 mA. With smallest cathode groove $t \sim 1 \text{ mm}$ and low gas density, it is possible to have a high efficiency of negative ion generation (80 mA for 10 A arc) because the ions emitted from cathode surface can penetrate the thin layer of plasma without destruction. But the brightness of this beam is not too high. By increasing a filter deepness d and the gas density, it is possible to transform the accelerated negative ions from the surface into the flow of cold negative ions with a high density. The brightness of the beam generated in

this regime is close to the brightness of the beam from SPS with Penning discharge ($j/T=1 \text{ A/cm}^2 \text{ eV}$), and the efficiency of beam generation is approximately the same also. The semiplanotron is good for stable operation in noiseless regime with production of H⁻ beam $\sim 0.1 \text{ A}$. With pulses 0.25 ms wide, operation without special cooling is possible up to 50 Hz . In the optimized regime for beam of 0.1 A the typical extraction temperature is $T_y < 1 \text{ eV}$, $T_x \sim 3 \text{ eV}$.

With a noisy discharge, one observes the increasing of the effective ion temperature in the beam after extraction to high level. This heating of the beam can be suppressed by the addition of gas in the beam [5, 22]. The effective ion temperature recalculated to the emission surface, T_x can be $\sim 1 \text{ keV}$, much higher than the real ion temperature in discharge. By the expansion of the beam from transverse size d up to a , the local ion temperature must be reduced by the factor $(a/d)^2$ to meV level. A fluctuating electric field can stop the cooling at a higher local ion temperature. This ion temperature is low also, but after recalculation to the emission surface by factor $(a/d)^2$ it has a higher level. This “overcooling” initiated the “overheating” of strongly expanded beams. In the direction along the emission slit, with parallel trajectories and not too small local angle width, the sensitivity to fluctuations is not too high, and maintaining a low ion temperature is more easily realized. The fluctuation of the emission current density induces the moving of the emission surface, and fluctuation of the angle divergence. It also initiates transients in the process of space charge compensation by positive ion. The oscillation of positive ions in the space charge potential can lead to a strong magnification of fluctuating electric fields by the collapsing of the local concentration of positive ions. The potential energy of positive ions created in different positions in the quasi-parabolic space charge potential can be transformed into a high increasing in the local ion density and into magnification of fluctuating electric fields by positive ions. The increasing of the gas density and the accumulation of electrons in the beam help to suppress this strong fluctuation of the electric field and to suppress the strong heating of ions.

Practically, it is very important to use fast gas valve for fast injection of gas into discharge chamber and have triggering of discharge before the big escaping of gas through emission hole. Fast electromagnetic valve developed in Novosibirsk INP [25] is used for noiseless high current density H⁻ beam production. This valve used also in BNL magnetron. It is important to note that there is a strong suppression of the gas and cesium flow from the emission slit by the high density plasma of the discharge. Gas flux suppression by discharge is illustrated in **Figure 25**. Suppression of cesium flux by discharge is shown in **Figure 26**. The coextracted electron current is comparable to the ion current. This SPS can operate stably with noiseless discharge and generate an H⁻ beam with high brightness.

The ion beam is very parallel along the slit, with some divergence near the ends of slit, and has the regular angle divergence $\alpha_x = A x$ in the perpendicular direction x . This divergence depends on the relation between emission current density j_0 and extraction voltage U_{ex} . In the noiseless regime the current/radian has a sharp maximum near the optimal relation between these parameters, as shown in **Figure 23**. With a noisy discharge this dependence is more monotonic, and the magnitude of current/radian is much smaller.

For the beam focusing was used 90° bending magnet with central trajectory radius 8 cm or 5 cm, and with gradient index close to 1. The regular divergence can be decreased by focusing to $A < 10 \text{ mrad/cm}$. For measurement of the beam characteristics, an emittance scanner with two small holes ($S_1 = S_2 = 0.1 \text{ mm} \times 0.1 \text{ mm}$) separated by $L = 205 \text{ mm}$, has been used as shown in **Figure 19**. Two perpendicular electrostatic deflectors can be calibrated by moving of ion jet on the surface of a luminescent screen with scale. This system may be used for direct registration of a local level of a four-dimensional brightness of ion beam. The beam quality is very well indicated by the magnitude of current to the collector after the second small hole.

With a noisy discharge, the effective ion temperature in a beam of 0.1 A in the direction along the slit was $T_y = 10 \text{ eV}$. For the perpendicular direction (along the magnetic field) the effective temperature was $T_x = 0.3 \text{ keV}$. For a noiseless discharge, but with excitation of fluctuations in the ion beam, it was possible to have $T_y = 2 \text{ eV}$ and $T_x = 15 \text{ eV}$ (beam current 0.1 A). From discharges with generation of 18 MHz RF , the effective ion temperature was up to two times higher. After optimization, and suppression of fluctuations in the transported beam, the characteristics were improved up to $T \sim 1 \text{ eV}$, $T_x \sim 5 \text{ eV}$ for $I = 80 \text{ mA}$ ($j = 1.6 \text{ A/cm}^2$). The best results were obtained with small beading magnet ($R = 5 \text{ cm}$): $T_x, T_y < 1 \text{ eV}$ for $I = 40 \text{ mA}$ ($j_0 = 0.8 \text{ A/cm}^2$). Some details of these experiments are presented in References [25-29].

If the discharge is noiseless the negative ion beam can still be noisy through excitation of instabilities. A strong instability can be excited by secondary electrons, entering the beam from solid surfaces if the beam hits it. The excitation of this instability is demonstrated in **Figure 27**. The upper trace is the signal from the negative ion beam collector, grounded by 100Ω resistor.

The lower trace is the signal from a shielded electron collector with negative potential, located near the beam. Initially, the negative space charge of the beam suppresses secondary electrons, but oscillation of the signal is observed. After compensation of space charge and overcompensation, a strong instability was excited, which lead to the fast removal of compensating particles from the beam. This stops the instability, and allows the accumulation of secondary particles again, which repeat the instability excitation. This instability induced a strong heating of the ion beam also.

The noiseless beam can be stable if the emission of secondary electrons into the beam is suppressed and the gas density is not too high. But energy dissipation by oscillating compensating ions is very low, and all disturbances (for example, micro breakdown in the extractor, from insulator or from insulating film) can excite the long “ringing”. Only after suppression of all causes like this is it possible to have a really stable noiseless ion beam with the highest brightness and good preservation of the ion temperature to lower then 1 eV . In this case it is also important to have the optimal relation between emission current density and extraction voltage, to prevent “overheating through overcooling”.

Finally, the noiseless cold beam does still have noisy microstructure. The measurement of current density by a collector with a small hole has shown high frequency fluctuation, as in **Figure 28**. The relative level of this noise is higher for a smaller hole (down to 0.1 mm) and grows along the beam. The noise is smaller if the slit

with collector is used and the slit is perpendicular to the magnetic field. It looks like a separation of the ion beam into very thin slices (flat fragmentation). The reason for this behavior of the beam is not yet understood.

The example of successful noiseless mode operation of SPS has been presented in paper of Moscow INR [30]. The P_{eff} listed in Table 1 show the magnetron, semiplanotron and Penning H^- SPS are the most efficient producers of H^- ion beams. P_{eff} is typically 15 times greater than pure H_2 volume production a factor of 7-8 more efficient than cesiated large volume SPS and approximately three times more efficient than the H^- large volume surface converter sources.

Lifetimes for the BNL and FNAL magnetrons are 6-9 months up to (3.6×10^8) pulses), while the comparatively longer *df* ISIS Penning has a lifetime of up to 50 days (2×10^8) pulses). Data presently presented for scaling of on magnetron and Penning H^- sources suggest they may be extended to the 100 mA, 5% *df* (50 Hz, 1 ms) range. A 4X Penning SPS from LANL was tested for production of 250 mA H^- current pulse at an arc discharge *df* of 0.5%. The LANL 4X source is scaled a factor of four in two of the three spatial dimensions as compared to the LANL 1X source. Measured 1rms normalized emittance is 0.15 ($\pi\text{mm-mrad}$) (narrow slit dimension) by 0.29 ($\pi\text{mm-mrad}$) in the long slit dimension for an unoptimized slit extraction system at 29 keV extraction energy. A magnetron scaling calculation shows that the BNL magnetron may be extended to 4.6% *df* at 100 mA H^- current with existing cooling. The lifetime of SPS is determined by electrode sputtering and flake formation. Cathode and anode sputtering are dominated by back accelerated positive ions. Suppression of back acceleration of positive ions should suppress cathode and anode sputtering. Improved cathode and anode cooling is necessary for increased discharge pulse length and intensity.

Optimized cesium film recycling (deposition-desorbition) could be used for shielding of electrodes from the sputtering and can reduce the sputtering to a very low level. Cesium in the SPS acts as an oil in an engine, increasing the operational lifetime. "Cold Start" of a discharge without cesium for a few minutes could be more destructive than many hours of low voltage operation. Electron emission from discharges without cesium is very high. An optimized extraction system with a suppression electrode should improve the beam intensity, beam quality and beam space-charge neutralization with a low gas pressure. A suppression of a back accelerating of the positive ion should suppress cathode and anode sputtering by accelerated positive ions - a main reason for the shorting of ion source lifetime. Improved cathode and anode cooling is necessary for increased discharge pulse length and intensity. The Semiplanatron version of the SPS can be the best one for operation at higher duty factor.

CSPS for DC operation.

Compact SPS for DC operation was developed in ref. [38]. Upgrading of this version of DC CSPS was presented in [39].

A basic configuration of this SPS is shown in *Figure 29 a*. Some modifications are presented in Fig. 29 b and 29 c. A glow discharge in the magnetic field is supported by a voltage between the cathode (1) and anode (5) separated by a ceramic insulator (4). The diameter of the cylindrical cathode body is 16 mm. The discharge, localized in the cylindrical channel of the hollow cathode (6), is 3 mm in diameter. The working gas (H_2)

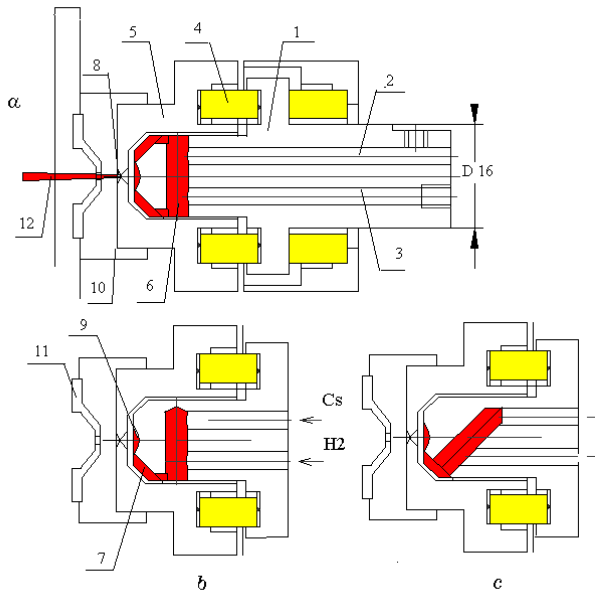


Figure 29. Modifications of the Hollow Cathode Discharge region in a compact DC SPS. *a* - perpendicular channel open on both sides; *b* – closed perpendicular channel; *c* – closed 45-degree channel.



Figure 30. Photograph of CSPS for DC operation: left- anode with emission aperture; right- cathode with cesium oven.

is delivered to the hollow cathode region through channel (3) from the gas system. The gas flow and pressure is controlled by a mechanical leak. Cesium is delivered to the discharge region through channel (2) from a small oven filled with pellets of cesium chromate and titanium powder mixture. Heating evolves a pure cesium vapor from the mixture. The plasma drifts in the crossed field (ExB) along the groove (7) to the spherical surface of the emitter (9). The direction of the plasma drift is determined by the direction of the magnetic field. The emitter's surface (9) is bombarded by positive ions and

neutrals from the plasma. Secondary negative ions, emitted from the spherical surface (9) are accelerated by the near surface potential well, without space charge limitation, and focused to the extraction aperture (8) with diameter of 0.3 to 1.2 mm. A beam of negative ions (12) is extracted by a high voltage applied between the anode (5) and extractor (11). A magnetic field, formed by permanent magnets, is between two poles (10). During operation this ion source is located in a vacuum chamber so the SPS parts don't need special vacuum sealing. The axial design simplified machining, assembling and maintenance of this SPS. A photograph of this SPS is shown in **Figure 30**.

Operation of this SPS was examined in the beam line test. Two or three electrode extraction optics with a suppression electrode was used for beam formation with a solenoidal magnetic lens for final focusing. Beam diagnostic was a moving beam collector for intensity, luminescent screens of ruby ceramic for source beam observation, and a quartz or YAG single crystal with a CCD camera for fine beam observations. Magnetic deflectors were used to manipulate the beam. An emittance scanner was used in early tests for emittance measurement. The first SPS was a configuration from Fig.29 a: a hollow cathode channel opens from on both sides. The focusing spherical radius was $R=3.5$ mm. With only hydrogen gas the discharge voltage was 0.4-0.5 kV so sputtering and flake formation was significant. After adding cesium, the discharge voltage dropped to 100 V and below. Stable DC operation has been reached with optimized heating of the cesium oven. In the previous tests [38] up to 2.5 mA of H^- was extracted through an extraction aperture of 1 mm diameter with a discharge voltage of 80 V and a current of 0.8 A. The emittance (90%) of a 25-keV H^- beam was $\varepsilon=26 \pi$ mm mrad. The estimated transverse ion temperature on the extraction surface is $T_i \sim 3$ eV. An effective brightness, $B=j/T_i=0.1$ A/cm² eV, was relative high, but 10 times smaller than for a pulsed SPS. For the beam line test the extraction aperture of 1 mm diameter was closed to 0.2 mm stainless steel foil with aperture 0.3 mm. With this aperture the H^- current in a remote collector after the solenoid lens, collimator and analyzer was 1 microamp, similar to the proton current from a Duoplasmatron (3 microamp). After 20 hours of operation the collector current started to increase and was 8 microamps after 60 hours. This current growth was due to an aperture increase by sputtering from back accelerated positive ions. With molybdenum foil this sputtering was invisible. In a clean vacuum an increasing current in extractor gap was observed, consisting of electrons and ions, independent of the gas and discharge. This emission was suppressed by a controlled leak of air. With a 0.3 mm extraction aperture the H^- beam was transmitted through the 8 m long 1 mm aperture beam line and final intensity was comparable with the proton beam from the duoplasmatron although repeatability of the H^- beam parameters was not stable. In the 29 a configuration a discharge can start from the top exit of the hollow cathode with a plasma drift to the right, to insulator (4), with a loss of ion emission. This loss of emission was the reason to change to configuration b with the hollow cathode opening on only one side, as shown in Fig.29 b. This version of the SPS was tested in another test stand with extending the operation of up to 4 weeks. This time was limited by the cesium in the oven. For longer operation a larger Cs supply is needed, as in the FNAL magnetron SPS [23]. For long operation is important to have at all times a low discharge voltage ($U_d < 90V$) and good Cs recycling. With a new anode and extraction aperture of 0.4 mm diameter an H^- beam up to 0.9 mA was extracted (emission current density $j=0.7$ A/cm²). The discharge voltage is $U_d=80$ V, discharge current $I_d=0.5$ A,

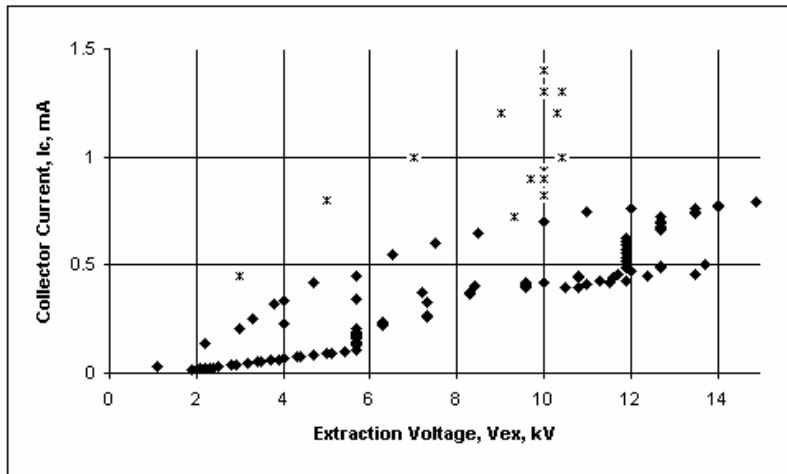


Figure 31. Dependence of H⁻ current on extraction voltage for different condition CSPS operation.

power $P=40$ W. The production efficiency at this current density. $F=j/P=17.5$ A/cm² kW, is much higher than $F=0.25-0.05$ A/cm² kW for a good proton source [9]. The next improvement is shown in Fig.1c. A hollow cathode channel was drilled normal to the conical part of the cathode surface and 45 degrees to the axis. This SPS minimized the distance for plasma drift to the emitter surface. The efficiency of negative ion generation has been improved. Dependence of the beam current at a test stand collector on the extraction voltage is shown in **Figure 31**. The collector current saturation is determined not by H⁻ stripping in the plasma, but by an increase of the cathode temperature and increased Cs desorption. A typical discharge voltage is $U_d=60-80$ V, discharge current up to $I_d=0.8$ A. Increasing the H₂ gas from $p=10^{-5}$ Torr to 3×10^{-5} Torr decreases the collector current from 1.4 mA to 0.5 mA. Traces of sputtering on the anode surface has conform good focusing of the negative ions by the spherical surface of the emitter. Moving the focusing point relative to the extraction aperture could change the intensity. Conditions for long time operation without any change in the parameters has been found.

With a two electrode extraction system a divergence of this high current density beam on the ruby screen was relative large ~ 50 mrad in agreement with a computer simulation by PBGUN code but aberration should be low and the brightness should be high. With an electrostatic Einzel lens after the extractor, the H⁻ beam can be transformed to a converging, parallel or a finely focused on the ruby ceramic screen.

A compact SPS for DC operation and a simplified maintenance is developed at Budker Institute of Nuclear Physics for a tandem accelerator of boron neutron capture therapy [40]. The source uses a Penning discharge with a hydrogen and cesium feed through the hollow channels in the cathodes. Discharge voltage is $\sim 60-80$ V, current ~ 9 A, hydrogen pressure 4–5 Pa, magnetic field 0.05–0.1 T, and cesium seed, 1 mg/h. Negative ions are mainly produced on the cesiated anode surface due to bombardment of hydrogen atoms. Negative ion beam current is directly proportional to the discharge current and to the

emission aperture area. A three electrode extraction system is used for the beam formation and acceleration. The current of coextracted electrons was suppressed by filter with transverse magnetic field. This electron flux was intercepted to the extraction electrode, biased at 4 kV potential with respect to the anode. An H⁻ ion beam with current up to 8 mA, beam energy 23 keV was produced. Current of heavy ion impurities had a value of about 3% of the total beam current. Beam normalized emittance is about 0.3π mm mrad and emission current density 0.1 A/cm^2 . A built-in cathode heater provides the quick start.

Compact SPS for heavy negative ion production is described in ref. [41]. This CSPA can be used for production of DC beam of B⁻ ions with current up to 0.9 mA from LaB₆ emitter with cesium admixture. Discharge in inverse magnetron with hollow cathode used for plasma generation.

LOW ENERGY BEAM TRANSPORT

The ion beam from a compact SPS has a very high current density ($j \sim 1-3 \text{ A/cm}^2$) and perveance. For transport of these beams it is necessary to use deep space-charge neutralization (compensation) or very strong continuous focusing by electrostatic forces as in the RFQ. Problems of H⁻ beam transportation were discussed recently in ref. [42]. Partial compensation of space charge with magnetic focusing and noisy beam will create a strong variation of focusing and lead to an increase of efficient emittance by emittance ellipse rotation. Still, this mode of transport is used in almost all injectors, and until recently it was acceptable.

A good solution could be a short LEBT with a fast beam over-neutralization by streams of noiseless plasma from a separate plasma source, or edition residual gas ionization by low energy electron beam.

SUMMARY

The CSPA have high plasma density, high emission current density. They are very small, simple and effective, have a high brightness in noiseless mode of operation, and high pulsed gas efficiency. The CSPA are very good for pulsed operation and continues operation during many months has been achieved. Negative ion formation, charge-exchange cooling of H⁻ below 1 eV, high brightness beam extraction, formation, transportation, space charge neutralization, brightness preservation instability dumping are discussed. Practical aspects of SPS design, simulation and operation, a gas pulsing and cesium admixture control, lifetime enhancement of selected SPS are described and compared.

Features of all discussed CSPA are small volume, small gaps between electrodes, high plasma density and high emission current density. These features have complicated the long time operation of CSPA with high beam parameters, because a sputtering rate, flakes formation, deposition of insulators surface and probability of short circuit of electrodes should be high. But in many versions of CSPA was reached a very long operation time.

The operation time of ion source is limited by cathode erosion in plasma, deposition of conducting films to the insulators and flakes formation with a short circuit of a discharge

gap between insulated electrodes. A typical current of DC discharge $I_d=1-10$ A is small enough for long time conducting by these short circuit. It was observed, than during operation of CSPS with a pulsed discharge with low impedance forming line a flakes formation is significantly suppressed and short circuit, created by deposition could be recovered. Short circuit created by conductive film deposition to the insulator or flakes can carry a low DC current but can be evaporated by high pulsed current. Evaporated material form a dust, accumulated in any pockets in gas discharge chamber without disturbing of discharge.

For prevention from conductive film deposition on the insulators it is possible to use for discharge operation a special power supply with pulsed mode of operation for pulsed evaporation of deposited films. Ion source should have a special volume (pocket) for collection and keeping of small flakes accumulated during long time operation. Ion source orientation should be suitable for flakes collection without disturbing normal ion source operation.

ACKNOWLEDGEMENT

The author is grateful of the colleagues Yu. Belchenko, G. Dimov, G. Derevyankin for cooperation in production of basic results, used in this work. I wish to thank Paul Farrell for useful discussions.

REFERENCES:

1. G.Budker, G. Dimov, V. Dudnikov, in Proc. Internat. Symposium on Electron and Positron Storage Ring, France, Sakley,1966, rep. VIII, 6.1 (1966), Sov. Atomic Energy, 22, 384(1967).
2. V. Dudnikov, The Method for Negative Ion Production, SU patent, C1.H013/04, No 411542, Appl. 3/10/72, granted 21 September, 1973, published in Bull. N0.2, 15 January 1974. Dudnikov "Surface Plasma method of Negative Ion Production", Doctor thesis, INP Novosibirsk, 1977.
3. Yu. I. Belchenko, G. I. Dimov, V. G. Dudnikov, "Physical Principles of the Surface Plasma Method for Producing Beams of Negative Ions," Proc. of the Symp. On the Production and Neutralization of Negative Hydrgen Ions and Beams, BNL 50727, Sept. 1977, Brookhaven National Labs. p.79.
4. V. Dudnikov, Rev. Sci. Instrum., 63(4),2660(1992). V. Dudnikov, Rev. Sci. Instrum., 73(2),992(2002). V. Dudnikov, PAC 2001.
5. V. Dudnikov, Proc. 4th All-Union Conf. On Charged Part. Accel.,Moscow,1974' V.1, p.323. Translated in LANL.
6. V. Dudnikov, PAC2001. Yu.Belchenko, G. Budker, G.Dimov, V. Dudnikov, et al. X PAC, Protvino, 1977.

7. C. Robinson, Aviation Week&Space Tech.,p.42, oct., 1978. Rev. Mod. Phys., 59(3), Part II,1987.
8. Nikita Wells, The development of High-Intensity Negative Ion Sources and Beams in the USSR, R-2816-ARPA,Rand Corp.,1981.
9. R. Scrivens, Proton and Ion Sources for High Intense Accelerators, EPAC 2004.
10. C. W. Schmidt, Prod. Neutralizat. of Negative Ions and Beams, 8th Internat. Symp. AIP 1-56396-773-5.1998.
11. H. Zhang, Ion Sources, Springer,1999.
12. J.Peters, Rev. Sci. Instrum., 71(2),1069 (2000).J.Peters, LINAC' 98, Chicago, 1998. J.Peters, EPAC'2000.
13. A.S. Belov, V.G. Dudnikov et al. Nucl. Inst. Meth. A333, 256-259 (1993).
14. A. Belov, V. Derinchuk, PAC01, 2001.
15. K.N. Leung, and K. Ehlers, R.S.I., 53, 803 (1982).
16. J. Ishikawa, Rev.Sci.Instrum., 67(3) 1410 (1996).
17. Y.Okumura, et al., Rev.Sci.Instrum.,71(2),1219 (2000).
18. Yu.I.Belchenko, V.I.Davydenko, G.I.Dimov, V.Dudnikov, Rev. Sci. Instrum., 61(1),378. (1990).
19. V.I.Davydenko, A.A. Ivanov, Rev.Sci.Instrum., 75 (5), (2005).
20. Joseph Sherman and Gary Rouleau, AARAI 02, Denton, TX 2002.
21. R. Welton, Linac,2002. (2002).
22. P.Allison, AIP Report No.158(1986)p.465.
23. C.W. Schmidt, C. Curtis, IEEE Trans. Nucl. Sci. NS-26,4120 (1979).
24. J. Alessi, Proc. of the 20th ICFA Advanced Beam Dynamics Workshop(ICFA-HB2002), Fermilab(2002).
25. G. Dimov, V. Dudnikov, G. Derevyankin, IEEE Trans. Nucl. Sci. NS-24,1545 (1977).
26. G.E. Derevyankin and V.G. Dudnikov, "Production of High Brightness H- Beams in Surface Plasma Sources", in Proceedings of the 3rd International Symposium on the Production and Neutralization of Negative Ions and Beams, BNL, 1983, AIP Conf. Proc. No. 111(1984), pp. 376-396.
27. G.E. Derevyankin and V.G. Dudnikov, "The Formation of the H- Beams for Accelerators Using of Surface Plasma Sources", Preprint 79-17, Institute of Nuclear Physics, Novosibirsk, 1979 (in Russian).
28. G.E. Derevyankin, V.G. Dudnikov and M.L. Troshkov, "Some Features of the H Beams Formation in Surface Plasma Sources", Preprint 82-110, Institute of Nuclear Physics, Novosibirsk 1982 (in Russian).
29. G.E. Derevyankin and V.G. Dudnikov, in Proceedings of the 4th International Symposium on the Production and Neutralization of Negative Ions and Beams, BNL 1986, AIP Conf. Proc. No. 158 (1987), p.395.
30. A. Belov et.al., Rev. Sci. Instrum, 63,2622 (1992).
31. J. W. G. Thomason and R. Sidlow, Proc. 7th European Particle Accelerator Conf., 1625(2000).
32. J. W. G. Thomason, et al., Proc. of the 20th ICFA Advanced Beam Dynamics Workshop (ICFA-HB2002), Fermilab (2002). J. W. G. Thomason, et al., Rev.Sci. Instrum, 75(5),1738 (2004). J. W. G. Thomason, et al., EPAC 2004.

33. Joseph Sherman, Gary Rouleau, et al., EPAC 2002, Proc. of the 20th ICFA Advanced Beam Dynamics Workshop (ICFA-HB2002), Fermilab(2002).
34. K. Leung, et al., AIP Conf. Proc.158, Edit J.Alessi, p.356, 1986.
35. K.Leung, et.al. Rev.Sci.Instrum., 58 (2),235 (1987).
36. Jones, Y.D., R.P. Copeland, and M.A. Parman, Proceedings of the Meeting, Los Angeles, CA, January 16-20, 1989. Bellingham, WA: Society of Photo-Optical Instrumentation Engineers, 1989, p. 573-577.
37. C.Schmidt, C.Curtis, AIP Conf. No158, p. 425 (1987).
38. A.Bashkeev, V.Dudnikov, AIP Conf. No 210, p.329, 1990.
39. V.Dudnikov, C.W. Schmidt,R. Hren, and J. Wendt, Direct current surface plasma source with high emission current density, , Rev. Sci. Instrum. 73 (2),989 (2002).
40. Yu. Belchenko and V. Savkin, Rev. Sci. Instrum., 75 (5), 1704,(2004).
41. V.Dudnikov, P.Farrell, Compact Surface Plasma Source for Heavy Negative Ion Production, Rep. PS5, ICIS 2003, Rev.Sci.Instrum, 75 (5), 1732,(2004).
42. I.A.Soloshenko, Rev. Sci. Instrum., 75 (5), 1694,(2004).